SEMI-ANNUAL PROGRESS REPORT

ON

NASA RESEARCH GRANT NGR 45 - 001 - 011

"Analysis and Interpretation of Magnetic Field Measurements Between Earth and Mars Received from Mariner IV"

Covering the Period

December 1, 1965 through August 31, 1966

Brigham Young University
Provo, Utah

October, 1966

I. INTRODUCTION

During the period of December 1, 1965 through August 31, 1966 the analysis being carried out at Brigham Young University has continued in the following areas:

1. The analysis of the near Mars magnetic field data.
2. A search for the extended magnetic tail of the Earth.
3. Geomagnetic fluctuations as observed at a number of ground stations and their relation to magnetic conditions in space.
4. The gross relationship of the interplanetary field configuration and geomagnetic fluctuation to M regions, sunspots, etc. on the sun.

Several papers presenting the results obtained to date under items 2, 3, and 4 are nearly completed and will be submitted for publication shortly. Consequently, we will only summarize briefly the results in these areas. A masters thesis covering a portion of the work under item 3 (daily averages of B and ΣK_p) has been completed and a portion is included herein.

II. FIELD MEASUREMENT NEAR MARS

A further study of the characteristics of the feature that occurred in the data starting at 0123 GMT, Day 196, has resulted in the following two conclusions:

1. There is no simple Martian field configuration that can be made to fit the data. If the feature is indeed of Martian origin, the variation in the field suggests that most likely the S/C passed into and out of the shock region, as the variability is not unlike some of those noted in the earth shock region.

2. Since a similar field signature was noted at approximately 27 days prior to that in question, this suggests that the feature under consideration was merely a fluctuation in the interplanetary field. In Figure 1 are plotted the 10 minute averages of the radial field component, B_R, and total field, B_{TOT}, for Days 196 and 223. Attention is called to the B_{TOT} feature occuring over the intervals 0130-0330 and 0700-0900 respectively, -- and similarly for B_R. Although the shapes of the features are different, the width and time separaration ($\sim$27 1/3 days) strongly suggest a time variable but persistent feature of solar origin. Equally of interest is the fact that for both periods the total field was relatively constant for a period of about 24 hours preceding the features of interest. If of solar origin, we hope to eventually relate these to the magnetic field topology on the surface of the sun (in cooperation with Professor L. Davis of C.I.T.).

III. A COMPARISON OF MARINER IV DATA WITH SOME ASPECTS OF LARGE-SCALE GEOMAGNETIC FLUCTUATIONS

The work reported in this section deals with large-scale disturbances observed during the period from launch, Day 333, 1964 to Day 70, 1965. The results have also been presented as part of a Masters Thesis by Keith H. Stirling (1966), one of the graduate assistants working on this project.

In order to demonstrate the general large scale correlation between the earth and interplanetary fields, daily averages of the Mariner IV data have been compared to both ΣK_p and A_p. Figures 2 and 3 show the daily relationship between ΣK_p, A_p, and the interplanetary magnetic field, B. Note that there exists almost a one to one relationship between the "peaks and valleys"

of the curves until about March 3rd. At the beginning of March the correspondence between A_p or ΣK_p and B became less clear. By March the approximate Earth-Sun-Probe angle had increased to about 10°. Therefore, the breakdown in correlations suggests that either:

1. Angles greater than about 10° usually contain streams of plasma from different solar disturbances, or
2. Changes in the storm structure have occurred after the storm passed the earth due to dispersion and the superposition of plasma events of different velocities.

Cross correlation indices were computed relating ΣK_p or A_p with the daily averages of the interplanetary field for the period November 30, 1964 through March 13, 1965. A major portion of the cross correlation analysis is presented in Table I. All tabulated intervals of confidence correspond to 95% certainty limits. Some of the significant results of our cross correlation analysis are as follows:

Both correlation coefficients between the probe data and the two disturbance indices (A_p and ΣK_p) for the month of December were the same (0.48). In January the correlations with A_p and ΣK_p were 0.86 and 0.78 respectively,--which are our highest values. For February 1 through March 3, the correlations of A_p and ΣK_p with the probe data being lagged behind the geomagnetic indices by one day were 0.72 and 0.65. The respective overall correlations with A_p and ΣK_p for the period of analysis (December 1 through March 3) were 0.54 and 0.55.

In order to incorporate the appropriate lag time due to the finite plasma velocity, the empirical relationship of Snyder et al (1963) relating plasma velocity and ΣK_p,

$$V_p(\text{Km/sec}) = 8.44\ \Sigma K_p + 330,$$

was used to determine the accumulative radial and rotational time lag of

disturbances between the Earth and the probe. The above formula enters only in computing the radial time lag since the angular velocity used in determining the rotational time lag is just the 27-day solar period. Actually, in performing this computation we are already assuming that the disturbance in the angle enclosing the Earth and the probe is uniform because the K_p indices recorded at the Earth are used in Snyder's formula to determine the plasma velocity in the vicinity of the probe. Because of the manner in which it was developed, Snyder's formula should yield fairly good results as long as a good relationship exists between interplanetary and geomagnetic variations. Figure 4 shows the expected time lag in hours per day of flight, where we are using Snyder's formula to determine radial time lag.

Cross correlation coefficients were then computed using the lag-time corrected data using the equation of Snyder, et al. The correlation coefficient was found to increase by 0.01 in magnitude with ΣK_p and remained the same with the A_p index for December. For January, however, the correlation coefficients with A_p and ΣK_p were reduced to 0.80 and 0.75 respectively. For the period February 1 through March 3, the coefficients were respectively 0.63 and 0.60 as compared to 0.40 and 0.44. Over the entire three-month period from December 1 through March 3, the correlation coefficients for A_p and ΣK_p with B were increased to 0.62 and 0.60 with the inclusion of lag-time correction as compared to 0.54 and 0.55 without.

A possible explanation for the above is that both January and February were magnetically active months and perhaps this would suggest why the A_p index gave a higher correlation with the interplanetary field than ΣK_p. Since the K_p index is related logarithmically to the disturbance, while the A_p index is proportional to the amplitude of the geomagnetic disturbance, with the correlation coefficient being a function of the average magnitudes of the two time series involved, the A_p index would be expected to yield a higher correlation

coefficient for periods containing large differences in magnitudes, (i.e., higher activity periods).

The good correlation between A_p and B has suggested that a linear relationship between them might exist. A straight line was least squares fitted to a scatter diagram plotting B versus A_p resulting in the expression

$$B\ (\gamma) = 0.18\ A_p + 3.37\ .$$

Coleman (1966) has suggested that the r dependence of B is somewhere between $r^{-1.1}$ and $r^{-1.2}$ and since the A_p indices during this period of time were higher over the last 1/3 of the data studied here (i.e., between 1 and 1.2 AU) some of the points for high A_p would be higher if reduced to 1 AU. Consequently, if the above equation were to represent the variation in B at the orbit of the earth, then the equation would be expected to have at least a steeper slope.

However, it is difficult, as in the case of V_p versus ΣK_p, to formulate a convincing argument why B should be correlated with A_p, unless one assumes that actually high B accompanies high variability in the interplanetary field, the latter being the real cause of geomagnetic activity (see Section IV).

IV. TRANSVERSE OSCILLATIONS IN THE INTERPLANETARY MAGNETIC FIELD: A REQUISITE FOR GEOMAGNETIC VARIABILITY

In the past few years new and illuminating aspects of geomagnetic storms have been described. Akasofu and Chapman (1963) have outlined in some detail the development of the main phase of the storm and its simultaneity with Polar Magnetic substorms. Furthermore, Akasofu (1965) in reporting the morphology of visual aurora describes the close correlation of auroral substorms to polar magnetic substorms. A primary conclusion of these researchers was that variations in pressure of the solar wind could not be related in a simple way to the increase of particle kinetic energy density of the ring current or of auroral particles. They suggested that some other intrinsic difference between

solar streams must exist. In the following paragraphs we will describe a distinguishing characteristic of solar streams and show that they are a requisite for occurrence of geomagnetic and auroral events.

Although the histograms of the interplanetary field show a definite spiral structure, when consecutive field lines passing a point in space are analyzed they present what at first appears to be a hopeless tangle of substructure. Hour means of the field components smooth the patterns considerably. Figure 5 displays the quantity $\left(\frac{dB\phi}{dt}\right)^2$ from these hour means and also the parameter K_p. $B\phi = \sqrt{B_T{}^2 + B_N{}^2}$ is the component of the interplanetary field in the plane normal to the sun probe line. In the third and forth segments of the record the K_p plot has been offset by the appropriate lag for the left margin of the figure.

Even though the geomagnetic activity is very low during this period and the probe moves some 12 million miles from the earth, there is a remarkable correspondence between the planetary magnetic variability and the magnitude of the transverse oscillations in the interplanetary field. In addition to the time difference between the earth and probe due to distance and angular separation, there is the dispersion caused by velocity fluctuations of the solar wind. Neugebauer and Snyder (1966) have shown a frequent pattern of velocity variation in individual solar streams. The velocities were often greater on the leading or western edge of a stream and decreased rapidly toward the trailing edge. If this kind of variation is true for the wind during the early part of the Mariner IV Flight, the remarkable correspondence evident in Figure 5 will be improved.

The two events of highest interplanetary field magnitude observed during the early part of the flight occured while the earth and probe were seeing very nearly the same solar winds. Furthermore, they are the only two events during this period with sudden commencement storms observed on the earth.

During the first and most intense event near January 21, the probe was still leading the earth by about 400 earth radii and was some 2,500 earth radii further out from the sun. By February 8, the time of the second large event, the earth had passed the probe so that it was now lagging by some 850 earth radii. Although not unique to these two events, transverse oscillations in the interplanetary field and their correlation with geomagnetism are so dramatically displayed during these times when the earth sun probe angle was very small that they will be used for illustration.

Hour averages of B_T, B_N, B_R, and B for these two events are shown in Figure 6 along with the values of K_p. The geomagnetic record has been offset with the appropriate lag for the beginning time of each disturbance.

In order to facilitate the discussion of this figure it is convenient to identify three periods in the geomagnetic record of each event. The periods are characterized as follows: (1) a sudden commencement followed by a one to two day period at high variability, (2) nearly a day when the geomagnetic field is rather stable, and (3) a several day period of high variability that starts abruptly, varies throughout, and slowly decays.

There are several significant features of the interplanetary field as they relate to these three geomagnetic periods. First of all, the total interplanetary field strength is increasing during period one, high and constant during the stable geomagnetic period and variable and decreasing during period three. High magnetic field alone does not mean geomagnetic variability. Also of great interest is the relation of the transverse components of the interplanetary field to these geomagnetic periods. In particular, B_T, the component in the ecliptic, oscillates and rapidly increases during period one, slowly reverses direction during period two, and then oscillates and decreases during the last period. In fact, B_T has the appearance on this scale of a damped wave during period three.

The results described above impose severe constraints on an acceptable theory of magnetic storms, aurora, etc. The necessity for a time variant property in the solar stream has been anticipated (Akasofu and Chapman, 1963; Dessler and Fejer, 1963; Desler and Walters, 1964; Patel and Dessler, 1966). However, very few proposed mechanisms would respond sensitively to transverse oscillation in the interplanetary field. The hydromagnetic coupling proposed by Dessler and Walters (1964) predicts that hydromagnetic waves are generated by the wagging of the earth's magnetic tail. The wagging is due to fluctuations in the direction of the interplanetary magnetic field relative to the solar wind velocity vector.

Axford et al (1965) have outlined arguments suggesting that the tail of the magnetosphere provides a mechanism for the injection of energy into the magnetosphere. More recently, Coppi et al (1966) conclude from an analysis of a collisionless pinch in the neutral sheet of the tail that an instability exists. They claim that the instability transforms magnetic energy into kinetic energy in a way suitable to explain the characteristic times of auroral and magnetic events. The transverse oscillations in the interplanetary field could easily perturb this unstable configuration.

V. THE MAGNETIC MORPHOLOGY OF SOLAR STREAMS AND ITS RELATION TO GEOMAGNETIC STORMS

Correlation studies are continually being carried out to relate solar phenomenon to geomagnetic storms. Both positive and negative correlations have been obtained and their interpretations are controversial. Very often as part of the study a particular class of solar events is isolated and the time interval between either the start of the event or its central meridian passage and the onset of the geomagnetic storm is interpreted as the travel time required for particles to reach the earth from the sun. However, even with interplanetary observations of the plasma velocity it has been extremely

difficult to relate individual solar events with a particular particle stream near the earth (Snyder and Neugebauer, 1964). In this section we use the results reported above as the basis for a model solar stream that can be used to successfully reinterpret the correlations and travel time obtained earlier. We have shown in section IV that:

1. Transverse oscillations in the interplanetary magnetic field are a requisite for geomagnetic variability.
2. There is often a period of about a day or more when geomagnetic activity is very low (designated 2 on Figure 6) even though the interplanetary magnetic field remains high. This quiet period is preceded and followed by a noisy geomagnetic period that occurs while the solar interplanetary field is relatively strong but changing in direction. It is also common to have a major event that does not show a region of stable strong field and therefore no geomagnetically quiet period.
3. Prompted by the observational results presented above we now describe two general classifications of planetary geomagnetic storms. These storm types, derived from the K_p index, indicate world-wide patterns of geomagnetic variability. Their characteristics are illustrated in Figure 7. For each type two examples are shown, a mean pattern from four years of geomagnetic records is given and a model is presented that accentuates the characteristic features. Although the patterns are seen throughout the solar cycle, the means are formed for years during minimum activity when the storms are more isolated. Eighty-one per cent of all sudden commencement storms from 1962-1965 are included in one of the two groups. In order to minimize personal bias in selecting a beginning time, only the

sudden commencement storms as reported by Lincoln (various issues of the J.G.R.) were used. Since the nature of the commencement itself is more likely related to variations in velocity of the solar wind than its magnetic properties and since there are no other established differences in the geomagnetic storms that follow, our model will not distinguish between commencement types.

The primary difference between types A and B is simply whether or not a distinct lull in geomagnetic variability occurs during the passage of a single solar stream. This has significant implications on the interpretation of the conventional geomagnetic storm which is described in terms of the time changes in magnitude of the various magnetic components. This subject will be discussed in a separate paper. In summary: Type A storms have two unequal periods of geomagnetic variability. The shorter first period of variability is followed by about a day of relative quiet and finally a longer period of slowly decreasing variability. Type B storms build rapidly to their maximum and though they range in variability, they slowly decrease with no distinct quiet period.

4. Bumba and Howard (1965) have obtained synoptic charts of solar magnetic fields. Although the patterns are complicated and continuously changing, it is possible to identify large unipolar regions that often persist for many solar rotations. Wilcox and Ness (1965) and Coleman, et. al. (1966) have described the extended portions of these unipolar regions as they are seen in interplanetary space as polarity sectors.

Within these broad unipolar regions there is a changing pattern of individual magnetic storms. The storms range from large, well-organized systems that dominate an entire sector to many small storms of a preferred polarity but with a tangled pattern of magnetism. In this section we will idealize a single, large unipolar magnetic storm. This model is essentially an extension of one discussed by Davis (1964). The solar gas rises most easily in the unipolar regions where the field lines are radial. The gas accelerates in the upper corona and streams outward retaining the polarity of the solar magnetic storm. Surrounding the uniform stream flowing out of this "magnetic nozzle" is a region of considerable irregularity in the field. Much of the irregularity is embedded in the plasma as it leaves the sun, but no doubt a significant amount is developed enroute as streams of different velocities interact.

Figure 8 illustrates a model storm in both a plane parallel to the ecliptic (a) and in cross section (b). Significant features of the storm are: (1) Two zones characterized by the intensity and variability of the magnetic field. The central high intensity region of the storm has parallel field lines. A second surrounding region has a disordered field. (2) An asymmetry in the pattern due to the spacial velocity distribution.

5. We now consider a persistent solar stream of the kind just described and investigate the appearance of magnetometer traces obtained during a crossing. The probe record illustrates the actual magnetic field of the stream whereas the earth responds to and we obtain a record of some quantity closely related to the time derivative of the interplanetary field. The maximum

velocity of such streams varies considerably. Snyder and Neugebauer (1963) obtained maximum speeds of 700-800 km/sec in 1962 and Wilcox and Ness (1965) report 350-450 km/sec speeds in 1963. The latter observations were obtained during solar minimum and likely represent the lower limit during the cycle. Compared with the motion of these streams, the motion of the earth or probe can be neglected. The probe (earth) is engulfed by the stream blowing outward. As the sun rotates, the stream moves across the probe (earth). In time, the probe (earth) sees the plasma along a path diagonal to the stream as suggested by D-D in Figure 8.

In Figure 9 the traces expected at the probe of the magnetic field are illustrated for the traversals B-B' and C-C' indicated in Figure 8. When the earth passes through the central part of the stream, we see a Type A Planetary Magnetic storm and when it passes through the edge of a stream we record a type B disturbance. It is important to stress that the type B trace will also be observed when passing through disordered regions due to many small solar streams.

On the basis of this model, we are able to account for the reported solar terrestrial correlations dealing with sunspots, flare events, centers of activity, M disturbances, and the wide dispersion of corpuscular speeds.

VI. THE MAGNETIC TAIL OF THE EARTH AND THE MOON

We have continued analyzing the data corresponding to passage of the S/C behind the earth near February 1. The quantity $\sigma B_{T,N}$ $\left(=\sqrt{(\sigma B_T)^2 + (\sigma B_N)^2}\right)$ has been found to follow closely variations in the terrestrial K_p index, and we have compared these two during the period of passage near the axis of the

earth's tail as well as preceding and succeeding periods in an attempt to detect any anomalous characteristics of the tail region. There is a suggestion that the level of activity at the probe was slightly lower than it should have been during the latter half of Day 30. Plotted in Figure 10 are both $\sigma B_{T,N}$ and K_p for Days 27 through 33, 1965.

There are several problems, however, with the assumption that the probe passed through the extended tail. First, the solar wind velocity that is required in order for the S/C to pass near the axis of the tail toward the end of Day 30 is $\sim$ 600 KM. The plasma velocity for this period, however, was nearer 350-400 KM/sec (Lazarus, et. al., 1966). Second, had the S/C passed through the tail, the measured radial component should have been inward or negative, while in fact it was directed outward, or positive. We are continuing to compare the characteristics of the interplanetary and terrestrial magnetic fields and as more of the respective characteristics correlate, we will continue to look at the tail and nearby regions.

No further work has been done on the data of $\sim$ 0800-1600 of Day 334 when the S/C was behind and below the moon. However, we have re-analyzed the data published by Ness (1965) corresponding to passage of IMP 1 behind the Moon during the period of December 14-15, 1963. Plots of K_p and $\sigma B_{T,N}$ are shown in Figure 11.

In these data there appears to be the same high degree of correlation of K_p with the three hour averages of $\sigma B_{T,N}$ that has been found to exist while the angular separation between the Earth and Mariner IV is small. (It should be noted that since these three hour $\sigma B_{T,N}$ values were computed from the hourly means, only the fluctuations in this general period interval are included. It has been found that if shorter period fluctuations are included in the sigma calculation, the correlation with K_p is usually much better.) We therefore conclude that the interpretation given by Ness to these data regarding

the Lunar Wake must be incorrect. Others have also suggested that his interpretation is uncorrect, (Greenstadt, 1965; Hirshberg, 1966).

VII. GEOMAGNETIC MICROPULSATIONS AND THE INTERPLANETARY FIELD

We have concerned ourselves here with giant geomagnetic pulsations ($T > 2$ min) that were observed at high altitudes during the early months of the Mariner IV flight. We are now able to describe many of the unique characteristics of the interplanetary field engulfing the earth when these pulsations occur.

Although the study is not yet complete, we now have sufficient evidence to show that:

1. Giant Pulsations occur when the interplanetary field is high and relatively stable.
2. Spectral analysis of the interplanetary field show that the component of the field normal to the ecliptic plane often peaks at the same frequency as that of the geomagnetic pulsations.
3. The power spectrum of the field observed by Mariner IV has a peak at the same frequency ($\sim$ 6 min.) as the power spectrum of the electron flux observations obtained by Imp. I in the distant earth field for the unusual event of Feb. 6, 1965, (Lin, et. al.). See Figure 12.

We are pursuing these exciting results and others at the present time.

VII. REFERENCES

1. Akasofu, S.-I., Dynamic Morphology of Auroras, Space Sci. Rev. 4, 498-540, 1965.

2. Akasofu, S.-I., and S. Chapman, The Cepartment of the Main Phase of Magnetic Storms, J. Geophys. Res., 68, 125-129, 1963.

3. Axford, W. I., H. E. Petschek, and G. L. Siscoe, Tail of the Magnetosphere, J. Geophys. Rev., 70, 1231-1236, 1965.

4. Bumba, V., and R. Howard, A Study of the Development of Active Regions on the Sun, Ap. J., 141, 1492, 1965.

5. Coleman, P. J., L. Davis, Jr., E. J. Smith, and D. E. Jones, Variations in the Polarity Distribution of the Interplanetary Magnetic Field, J. Geophys. Res., 71, 2831-2839, 1966.

6. Coleman, P. J., E. J. Smith, L. Davis, Jr., and D. E. Jones, The Radial Dependence of the Interplanetary Magnetic Field, J. Geophys. Res. to be published, 1966.

7. Coppi, B., G. Laval, and R. Pellat, Dynamics of the Geomagnetic Tail, Phys. Rev. Letters, 16, 1207, 1966.

8. Davis, L., Models of the Interplanetary Fields and Plasma Flow, Paper presented at the Conference on "The Solar Wind," Cal. Tech., April 1-4, 1964.

9. Dessler, A. J., and J. A. Fejer, Interpretation of K_p Index and M-Region Geomagnetic Storms, Planetary Space Sci., 11, 505-511, 1963.

10. Dessler, A. J., and G. K. Walters, Hydromagnetic Coupling Between the Solar Wind and Magnetosphere, Planetary Space Sci., 12, 227, 1965.

11. Greenstadt, E. W., Interplanetary Magnetic Effects of Solar Flares: Explorer 18 and Pioneer 5, J. Geophys. Res., 70, 5451, 1965.

12. Hirshberg, J., Discussion of Paper by N. F. Ness, "The Magnetohydrodynamic Wake of the Moon," J. Geophys. Res., 71, 4204, 1966.

13. Lazaras, A. J., H. S. Bridge, J. M. Davis and C. W. Snyder, Initial Results from the Mariner 4 Solar Plasma Experiment, submitted for publication in the Proceedings of the 1966 COSPAR meeting.

14. Lin, R. P., and K. A. Anderson, Periodic Modulations of the Energetic Electron Fluxes in the Distant Radiation Zone, J. Geophys. Res., 71, 1827-1835, 1966.

15. Ness, N. F., "The Magnetohydrodynamic Wake of the Moon, J. Geophys. Res., 70, 517 (1965).

16. Neugebauer, M., and C. Snyder, Mariner 2 Observations of the Solar Wind, 1. Average Properties, J. Geophys. Res., 71, 4469, 1966.

17. Patel, V. L., and A. J. Dessler, Geomagnetic Activity and Size of Magnetospheric Cavity, J. Geophys. Res., 71, 1940-42, 1966.

18. Snyder, C. W., M. Neugebauer, and U. R. Rao, The Solar Wind Velocity and Its Correlation with Cosmic-Ray Variations and with Solar and Geomagnetic Activity, J. Geophys. Res., 68, 6361-6370, 1963.

19. Snyder, C. W. and M. Neugebauer, The Relation of Mariner 2 Plasma Data to Solar Phenomena, paper presented at the Conference on "The Solar Wind," Cal. Tech., April 1-4, 1964.

20. Stirling, K. H., M. S. Thesis, Brigham Young University, 1966.

21. Wilcox, J. M., and N. F. Ness, Quasi-Stationary Corotating Structure in the Interplanetary Medium, J. Geophys. Res., 70, 5793, 1965.

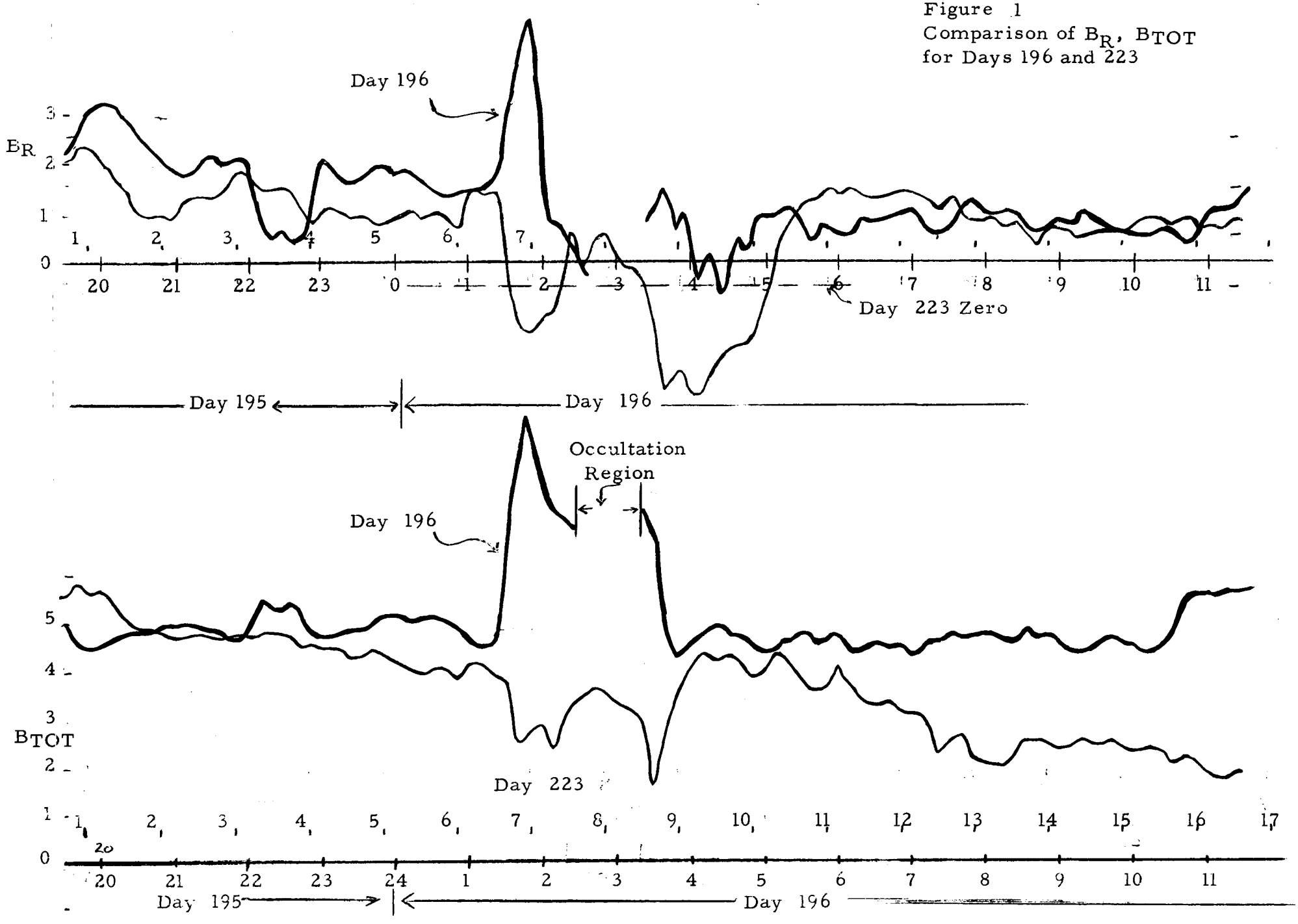
Figure 1
Comparison of B_R, B_{TOT}
for Days 196 and 223
Day 196
B_R
3
2
1
0
1
2
3
4
5
6
7
20
21
22
23
0
1
2
3
4
5
6
7
8
9
10
11
Day 223 Zero
Day 195
Day 196
Occultation
Region
Day 196
5
4
3
B_{TOT}
2
1
0
Day 223
1
2
3
4
5
6
7
8
9
10
11
12
13
14
15
16
17
20
20
21
22
23
24
1
2
3
4
5
6
7
8
9
10
11
Day 195
Day 196

RELATIONSHIP BETWEEN THE
INTERPLANETARY MAGNETIC FIELD
AND THE
Ap, ΣKp INDICES
(Part 1)

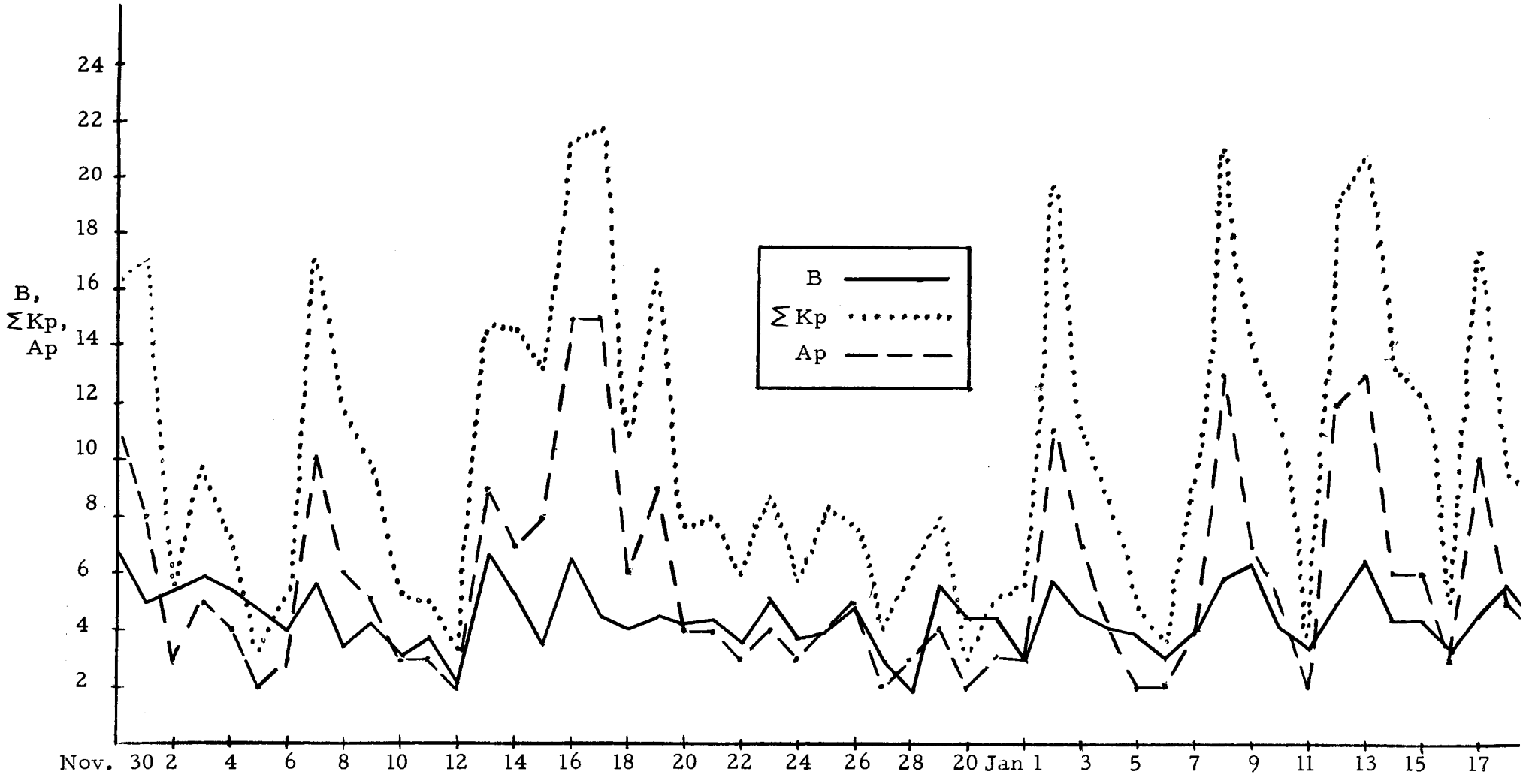

FIGURE 2

RELATIONSHIP BETWEEN THE
INTERPLANETARY MAGNETIC FIELD
AND THE
Ap, ΣKp INDICES
(Part 2)

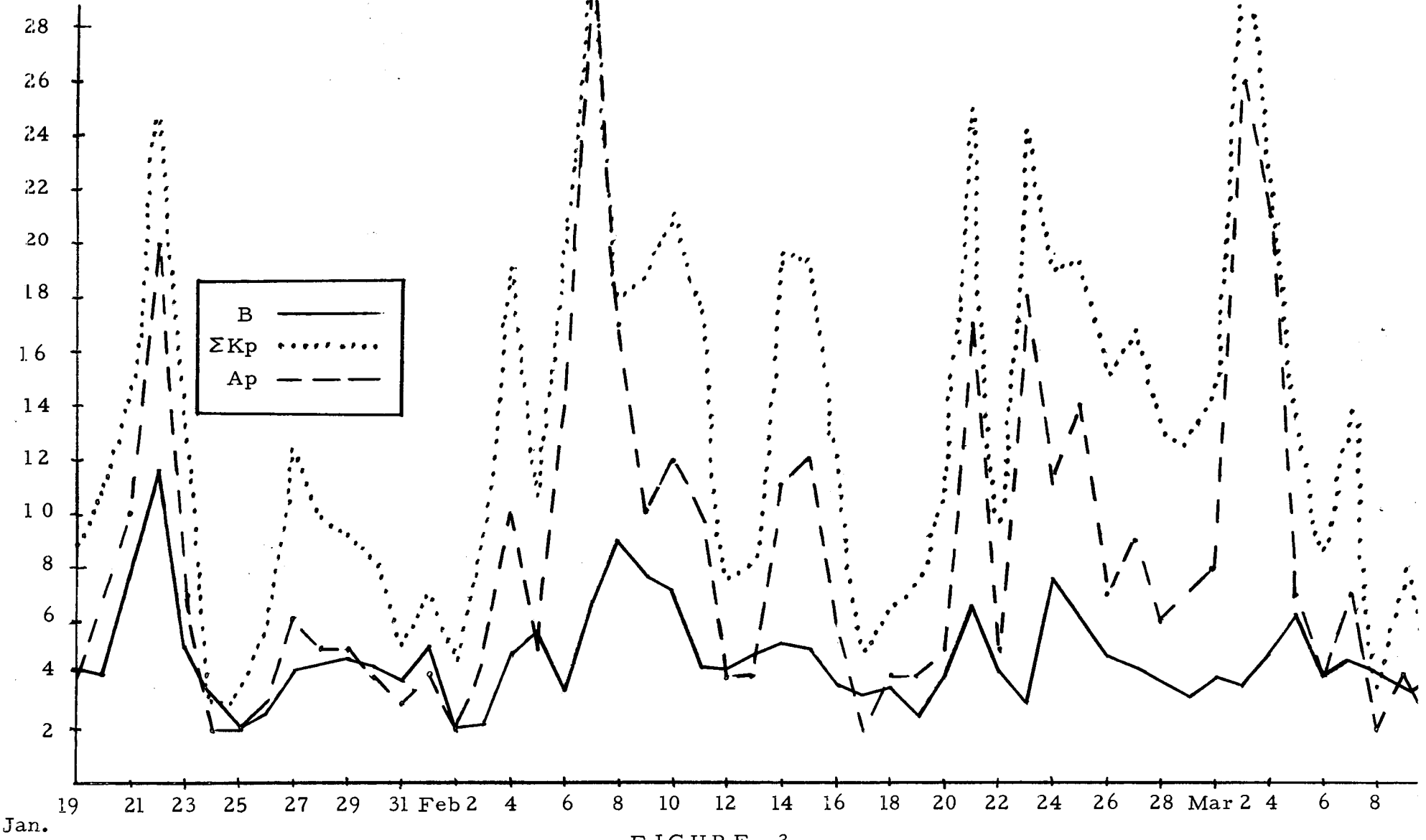

FIGURE 3

TABLE I

CROSS CORRELATION COEFFICIENTS

Period of Analysis	Time lag cor.	1st time series	2nd time series	Correlation for day preceding or following geomagnetic storm -5	-4	-3	-2	-1	0	+1	+2	+3	+4	+5	Confidence for underscored co.
12/1/64	No	ΣK_p	B	-.06	-.09	-.05	-.01	0.18	0.55	0.40	0.05	0.01	0.02	0.03	0.38-0.68
to	Yes	ΣK_p	B	-.10	-.06	0.00	0.05	0.31	0.60	0.21	0.04	-.06	0.04	-.01	0.45-0.72
3/3/65	No	A_p	B	-.15	-.11	-.02	-.03	0.13	0.54	0.47	0.13	0.04	-.02	0.00	0.37-0.67
	Yes	A_p	B	-.17	-.06	0.03	0.00	0.29	0.62	0.31	0.09	-.08	-.01	-.02	0.47-0.74
	Yes	A_p	BT	0.07	0.25	0.23	0.08	-.07	-.22	-.30	-.22	-.16	-.17	-.26	
	Yes	A_p	BN	-.05	-.11	-.14	-.04	0.06	-.38	-.23	-.04	-.10	-.06	-.11	
	Yes	A_p	BR	0.08	-.07	-.15	-.04	0.10	0.14	0.17	0.25	0.37	0.33	0.27	
*12/1/64	No	ΣK_p	B	-.22	-.03	0.32	0.08	0.07	0.48	0.04	-.02	0.01	0.01	-.18	0.14-0.71
to	Yes	ΣK_p	B	-.21	-.00	0.32	0.07	0.06	0.49	0.03	-.03	0.03	0.00	-.17	0.15-0.72
12/31/64	Yes	A_p	BT	0.25	0.32	0.14	-.09	-.31	-.28	-.27	-.27	-.23	-.15	-.23	
	Yes	A_p	BN	0.30	0.31	0.21	-.08	0.04	0.22	-.05	-.25	-.19	-.10	0.01	
	Yes	A_p	BR	0.09	-.24	-.07	0.19	0.46	0.40	0.49	0.31	0.35	0.26	0.11	
	No	A_p	B	-.30	-.02	0.34	0.09	0.07	0.48	0.03	-.07	0.04	0.01	-.17	0.14-0.71
	Yes	A_p	B	-.30	0.00	0.35	0.07	0.06	0.48	0.01	-.07	0.06	0.00	-.17	0.14-0.71
*1/1/65	No	ΣK_p	B	0.18	0.00	-.36	-.30	0.24	0.78	0.34	-.21	-.37	-.12	0.23	0.58-0.88
to	Yes	ΣK_p	B	0.17	-.12	-.40	-.16	0.43	0.75	0.10	-.25	-.37	0.07	0.12	0.53-0.87
1/31/65	No	A_p	BT	-.14	0.16	0.22	0.21	0.21	-.30	-.06	0.02	0.11	-.01	-.47	
	No	A_p	BN	-.27	-.33	0.08	0.23	0.58	-.07	-.22	-.00	0.04	0.28	-.06	
	No	A_p	BR	0.03	-.08	-.07	-.01	-.15	0.08	0.07	0.02	0.16	-.03	0.06	
	No	A_p	B	0.08	0.08	-.22	-.27	0.22	0.86	0.39	-.16	-.43	-.21	0.19	0.71-0.93
	Yes	A_p	B	0.13	-.04	-.24	-.21	0.48	0.80	0.18	-.25	-.45	0.00	0.10	0.62-0.90
*2/1/65	No	ΣK_p	B	-.32	-.45	-.09	0.07	0.14	0.44	0.65	0.18	0.20	-.01	-.22	0.37-0.82
to	Yes	ΣK_p	B	-.46	-.27	0.10	0.14	0.32	0.60	0.34	0.19	-.01	-.11	-.27	0.30-0.78
3/3/65	No	A_p	B	-.40	-.44	-.10	0.00	0.06	0.40	0.72	0.35	0.27	-.06	-.22	0.47-0.85
	Yes	A_p	B	-.49	-.26	0.04	0.05	0.25	0.63	0.51	0.30	-.03	-.16	-.23	0.35-0.81

*The 31-day time series have been lagged and led 16%, whereas the 104-day time series have been lagged and led 10% in the cross correlation program.

Figure 4 - Plasma Time Lag per Day of Flight

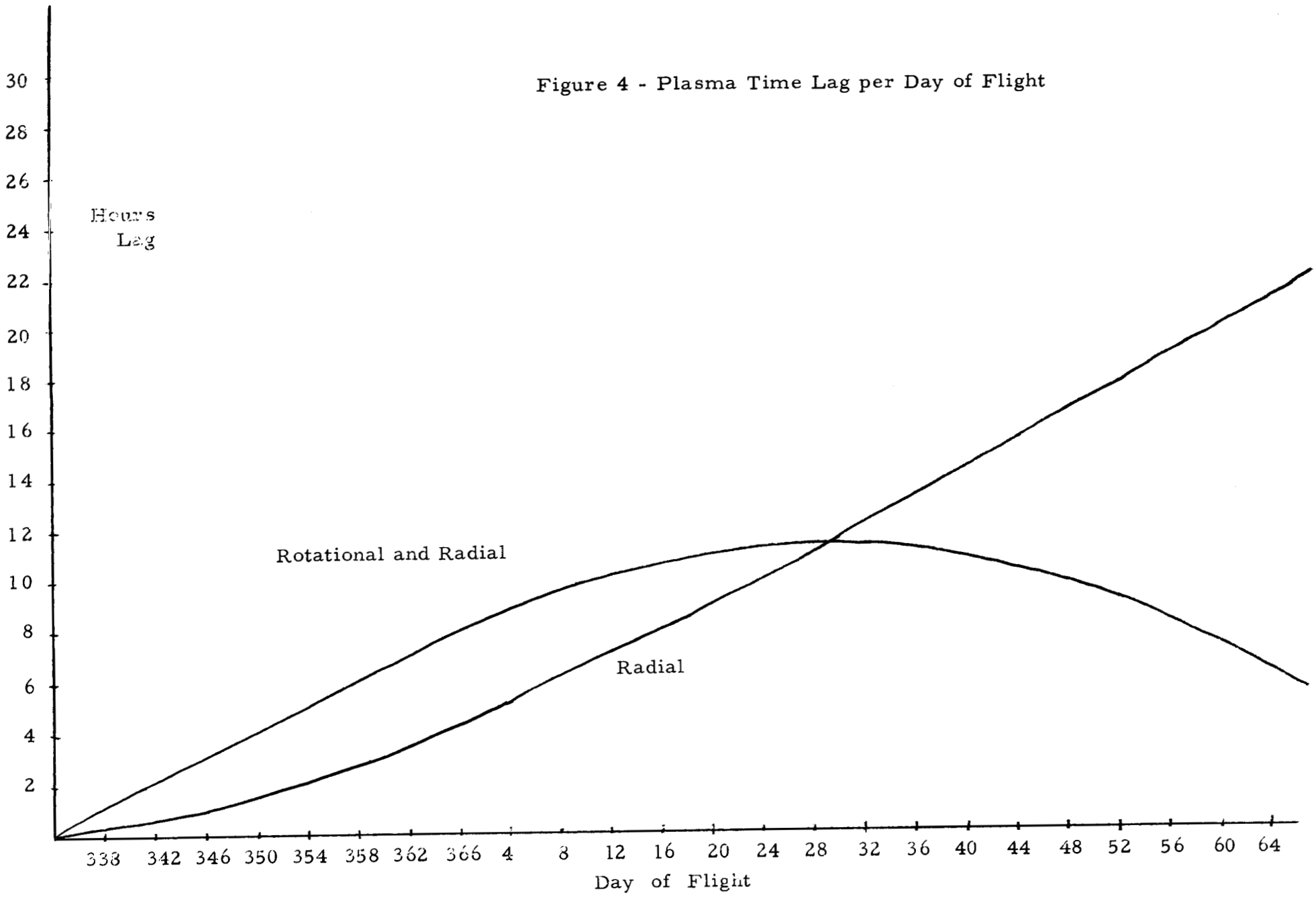

Figure 5 - Plots of $\left(\frac{dB_\phi}{dt}\right)^2$ and K_p

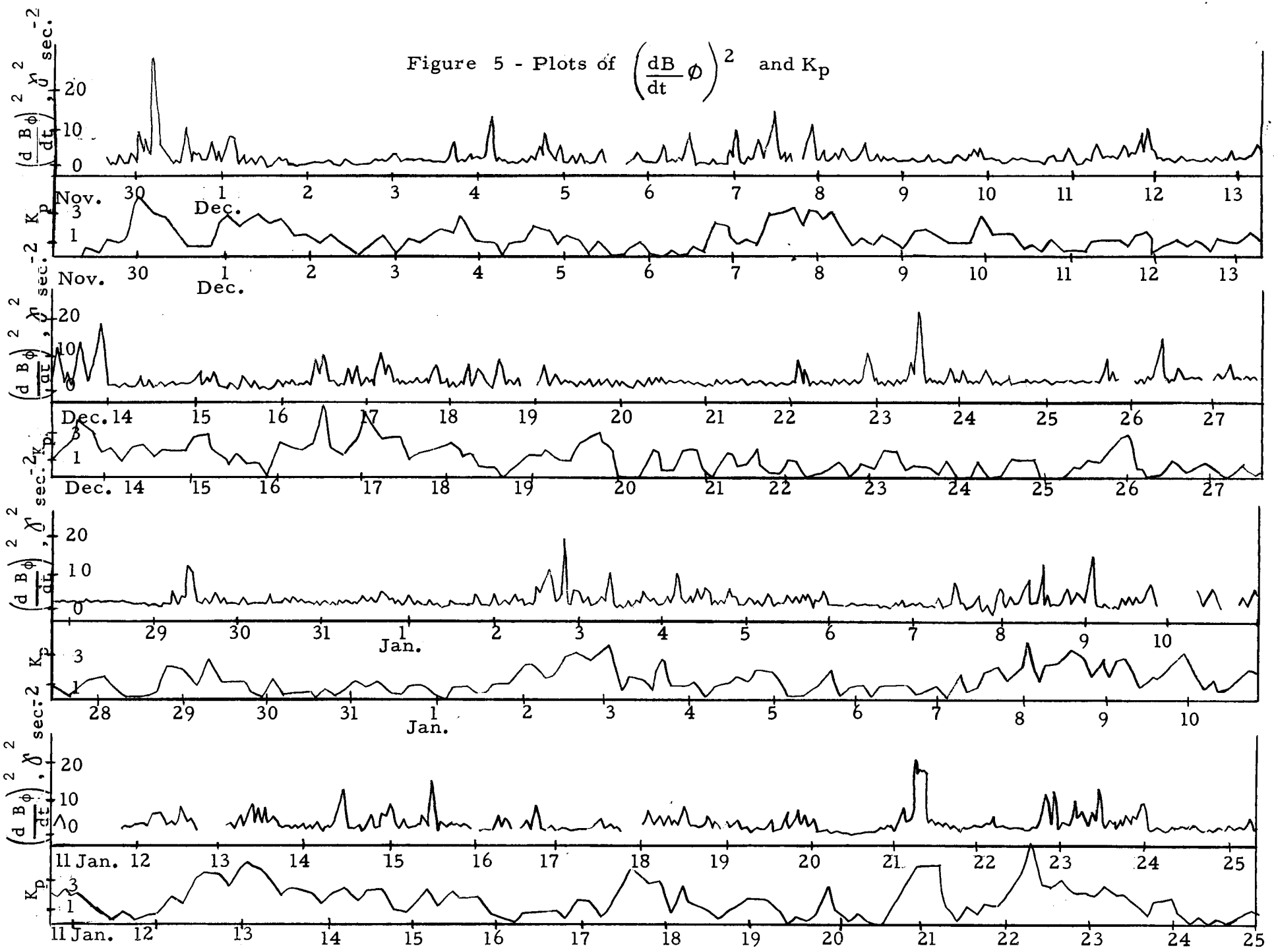

TIME, days

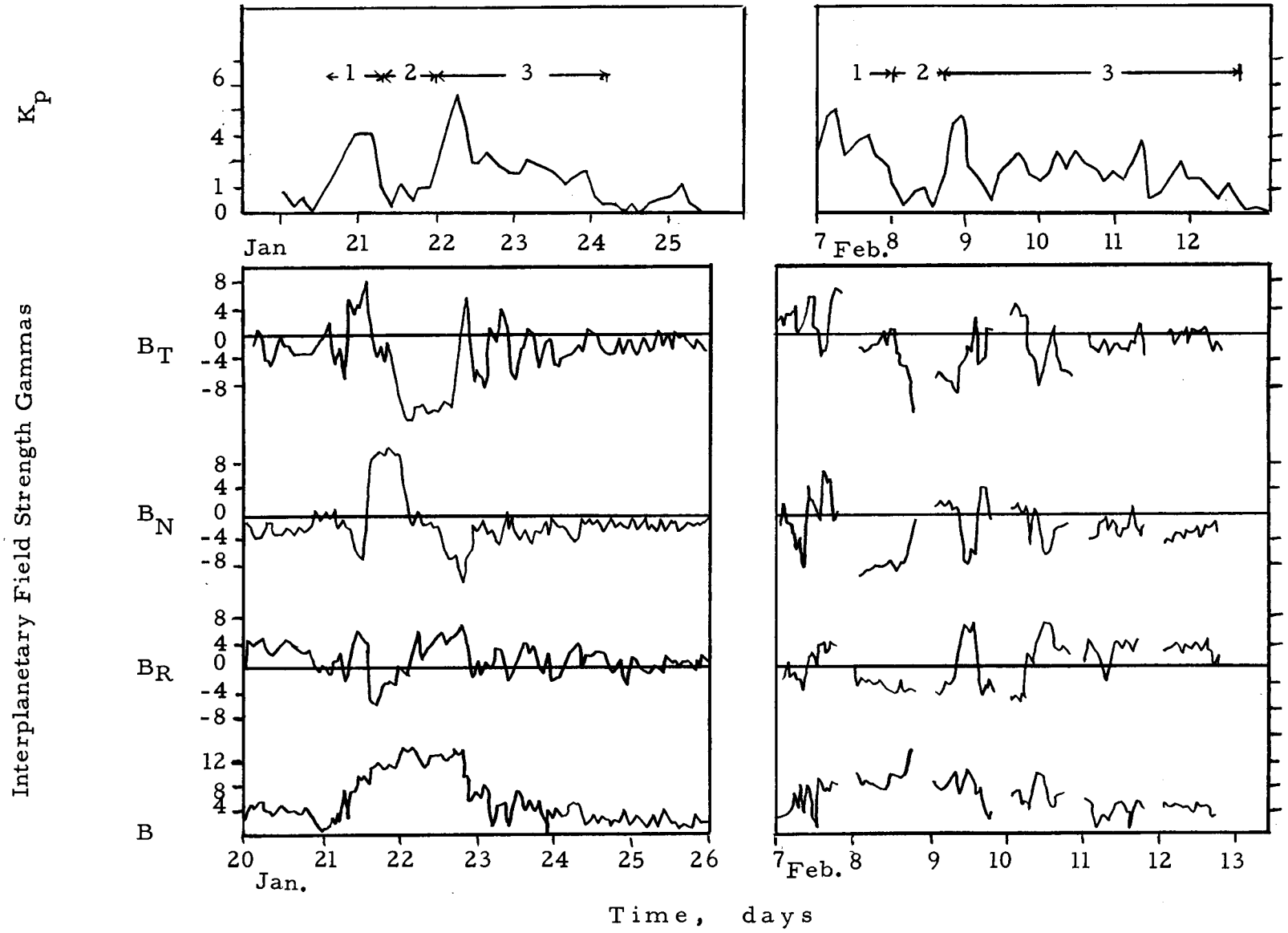

Figure 6 - Storms of January 21 and February 8

Figure 7

Type A

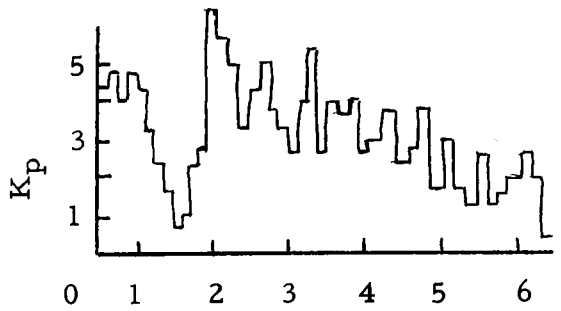

Example: S.C. July 24, 1962

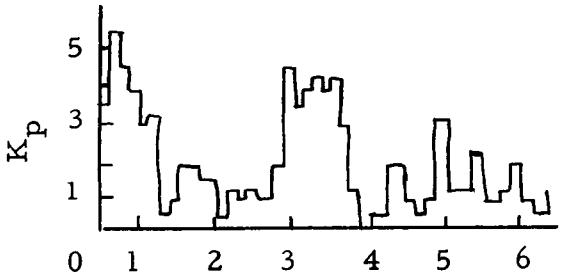

Example: S.C. February 4, 1962

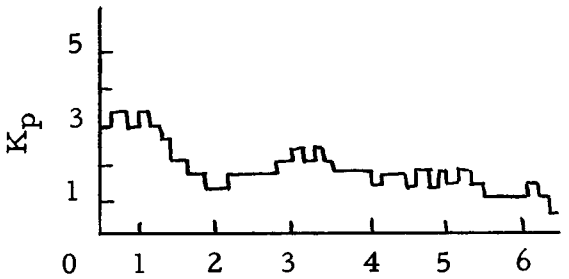

Mean K_p for 24 S.C. storms (45%) 1962-65

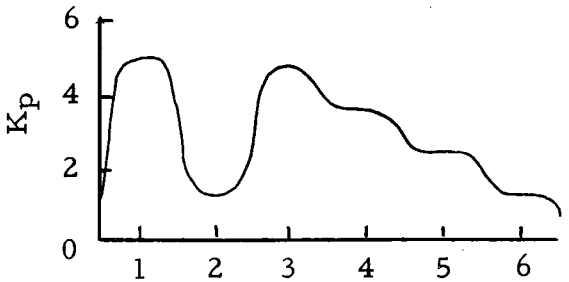

Model

Type B

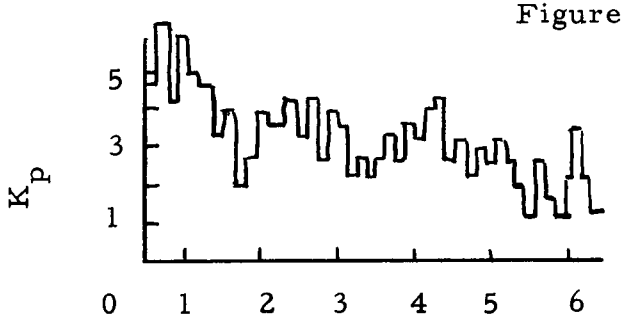

Example: S.C. April 30, 1963

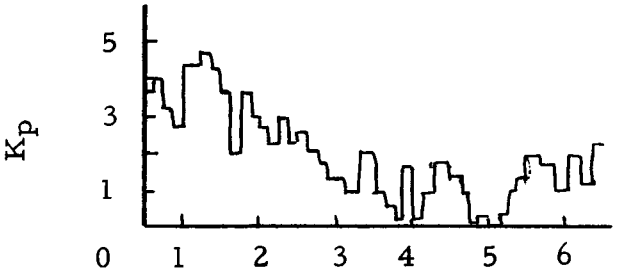

Example: S.C. August 11, 1964

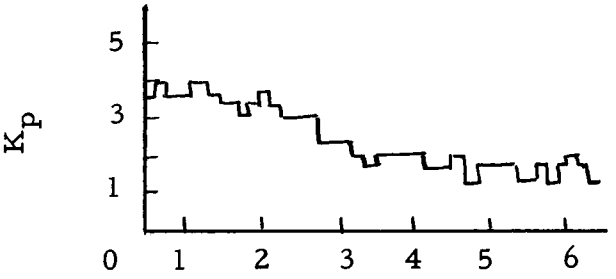

Mean K_p for 19 S.C. storms (36%) 1962-65

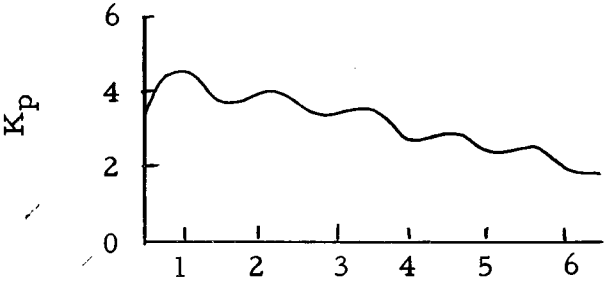

Model

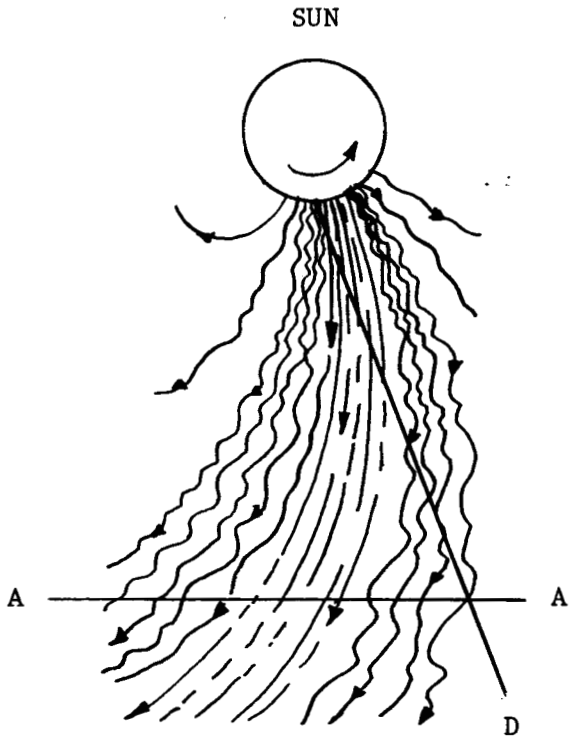

a. Field configuration in plane parallel to ecliptic

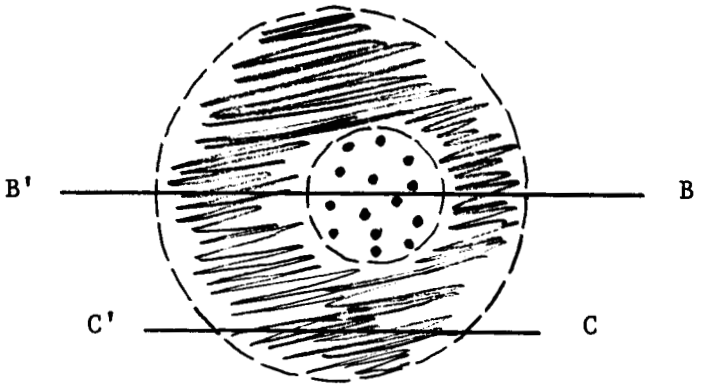

b. Field configuration in section A'-A

Figure 8

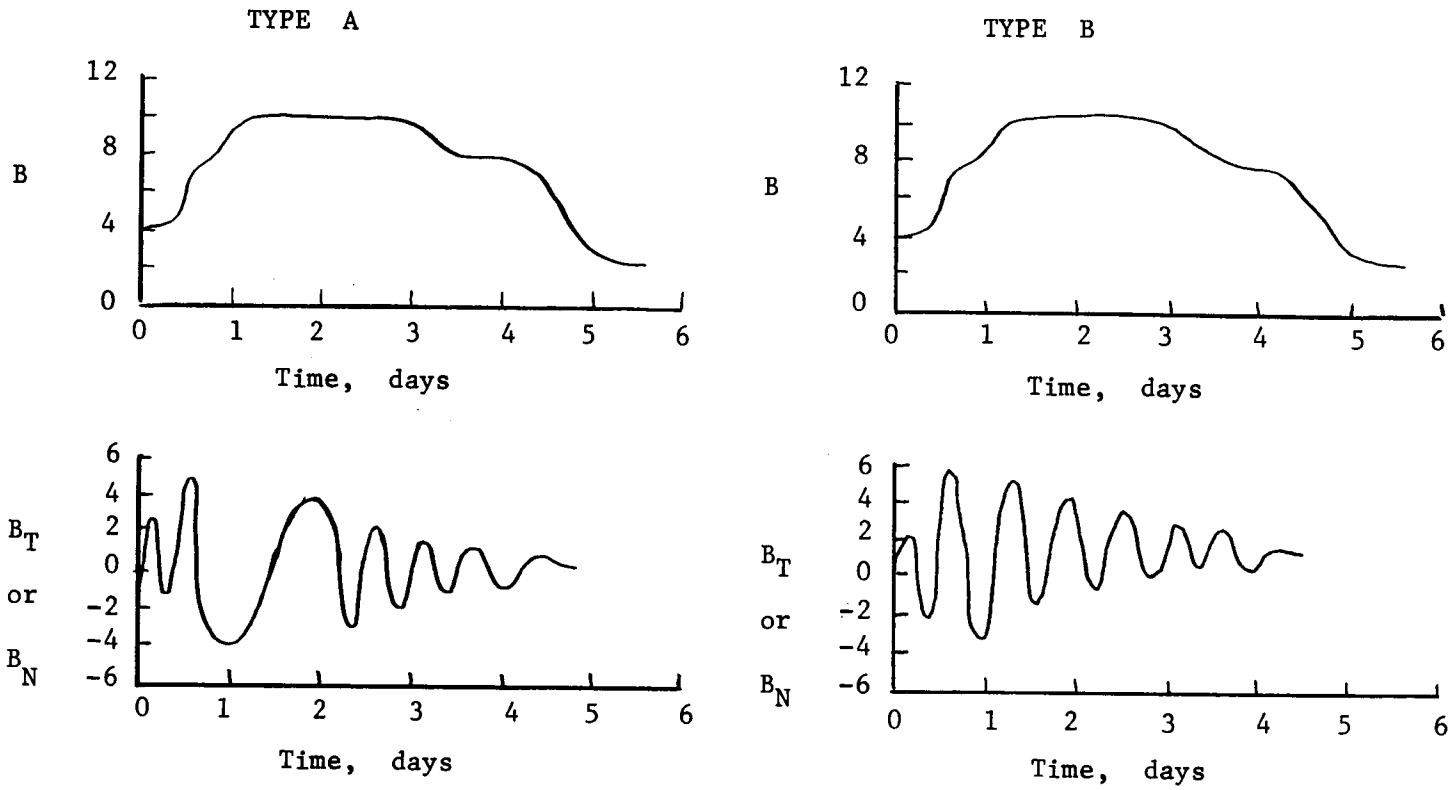
TYPE A
TYPE B
B
12
8
4
0
0 1 2 3 4 5 6
Time, days
B_T or B_N
6
4
2
0
-2
-4
-6
PROBE

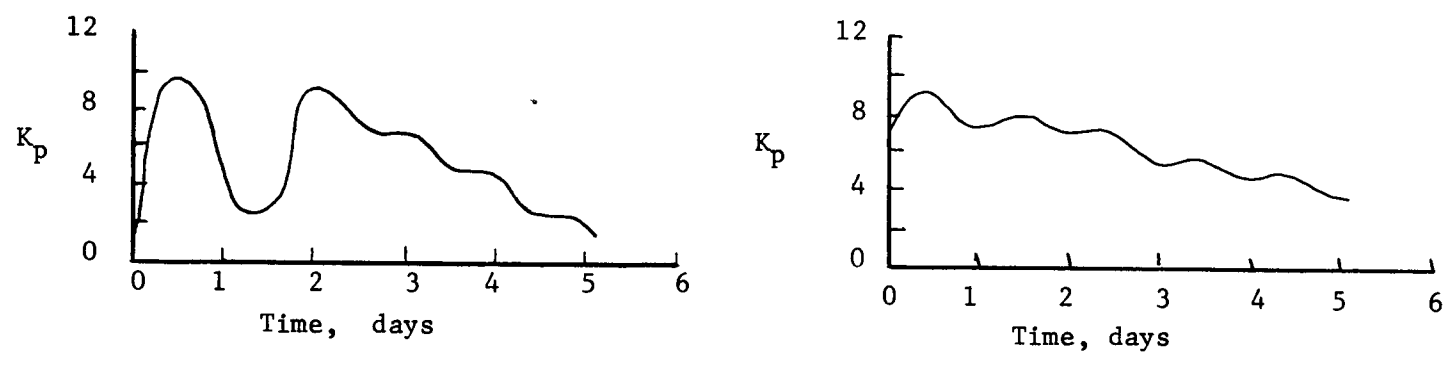
K_p
12
8
4
0
0 1 2 3 4 5 6
Time, days
EARTH

Figure 9

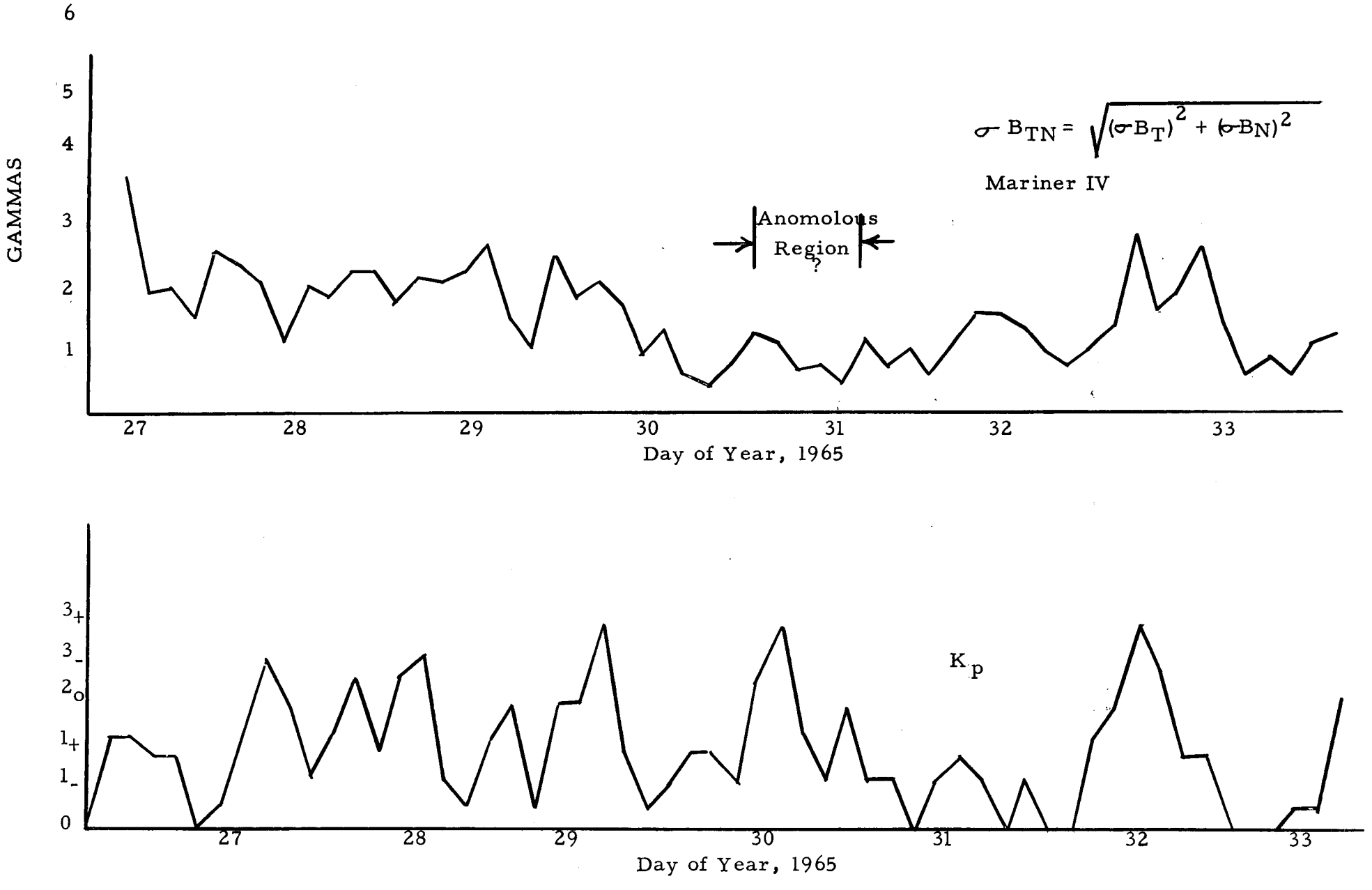

Figure 10 - Plots of σB_{TN} and K_p for Period Near February 1, 1965

Figure 11
Plot of σB_{TN} and K_p for period IMP 1 Behind Moon, (Dec., 1963)

$$\sigma B_{TN} = \sqrt{(\sigma B_T)^2 + (\sigma B_N)^2}$$

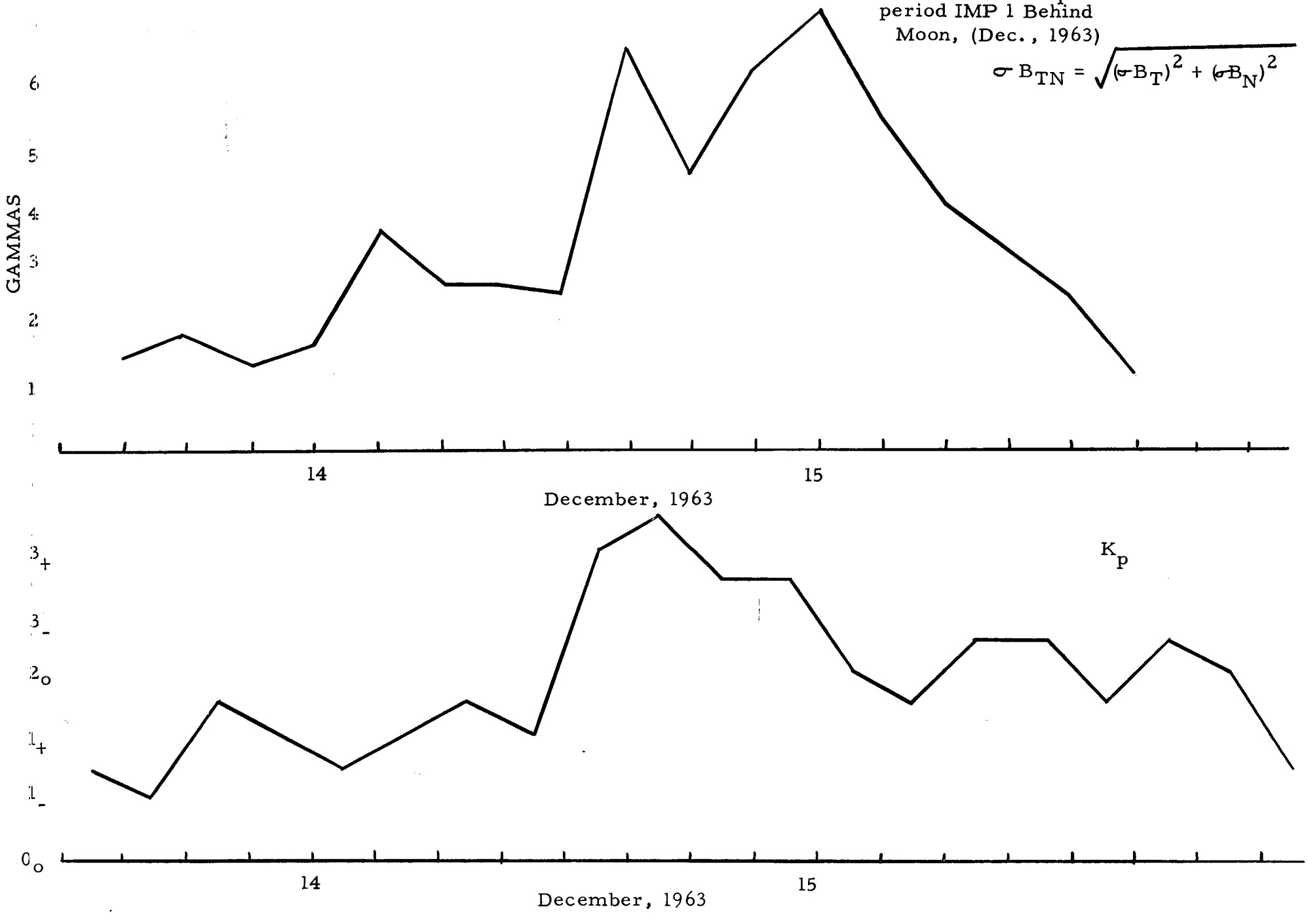

Figure 12

Power Spectra of Interplanetary and near earth conditions during a Geomagnetic Storm

(Note: A lag time of about 10 hours is required due to the greater radial distance to the probe.)

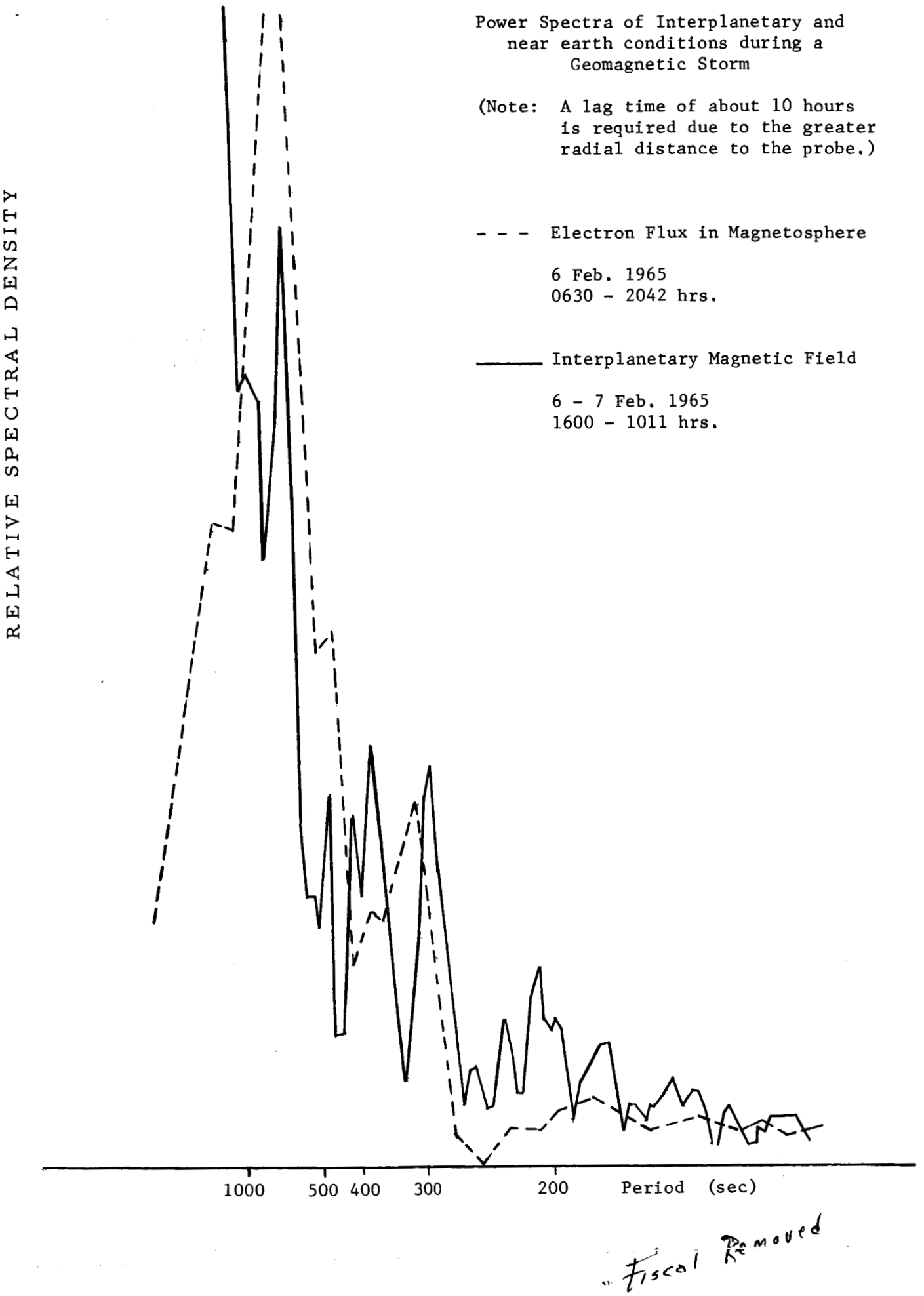

Fiscal Removed